JOURNAL OF Applied Polymer SCIENCE

Europium-Containing Cholesteric Liquid Crystalline Polymers in the Side Chain

Wen-Zhi Zhao, Yue-Hua Cong, Bao-Yan Zhang, Wei-Min Gu
Centre for Molecular Science and Engineering, Northeastern University, Shenyang 110004, People's Republic of China
Correspondence to: B. Zhang (E-mail: byzhang2005@126.com)

ABSTRACT: Europium-containing cholesteric liquid crystalline polymers were graft copolymerized using poly(methylhydrogeno)siloxane, cholesteryl 4-(allyloxy)benzoate (M_1), cholesteryl acrylate (M_2), and a europium complexes monomer (M_3). The chemical structures of the monomers were characterized by Fourier transform infrared and ^{1}H-nuclear magnetic resonance. The mesomorphic properties and phase behavior were investigated by differential scanning calorimetry, thermo gravimetric analysis, polarizing optical microscopy, and X-ray diffraction. With an increase of europium complexes units in the polymers, the glass transition temperature (T_g) did not change significantly; the isotropic temperature (T_i) and mesophase temperature range (ΔT) decreased. All polymers showed typical cholesteric Grandjean textures, which was confirmed by X-ray diffraction. The temperatures at which 5% weight loss occurred (T_d) were greater than 300°C for the polymers. The introduction of europium complexes units did not change the liquid crystalline state of polymer systems; on the contrary, the polymers were enabled with the significant luminescent properties. With Eu^{3+} ion contents ranging between 0 and 1.5 mol %, luminescent intensity of polymers gradually increased and luminescent lifetimes were longer than 0.45 ms for the polymers. © 2014 Wiley Periodicals, Inc. J. Appl. Polym. Sci. **2014**, *131*, 40866.

KEYWORDS: copolymers; liquid crystals; optical properties; thermal properties

Received 23 January 2014; accepted 13 April 2014
DOI: 10.1002/app.40866

INTRODUCTION

Cholesteric liquid crystalline polymers (ChLCPs) have attracted considerable interest because of the outstanding optical properties such as selective reflection and transmission of light, circular dichroism, and thermochromism.[1–3] Moreover, ChLCPs can form a stable Grandjean texture with selective reflection of visible light. In addition, heat resistance, good elasticity, and film-forming properties increase the potential application of side-chain ChLCPs, such as flat-panel displays, organic pigments, and full color thermal imaging. The structure of side-chain ChLCPs mainly contains the polymer backbone, the flexible spacer length and the rigidity of the mesogenic units.[4–6] At present, polysiloxane,[7] cyclosiloxane,[8] polyacrylates,[9] polymethacrylates,[10] and polyvinylethers[11] are usually used as polymer backbone for ChLCPs. To obtain the lower T_g and mesomorphic properties at moderate temperature, the polysiloxane backbone is usually used.[12] One of the strategies for synthesizing side-chain ChLCPs is graft copolymerized using polysiloxane, chiral LC monomers and additional monomers.

Rare earth luminescent materials are applied in many optical devices, such as displays, tunable lasers and amplifiers for optical communication.[13] Many rare earth complexes have been investigated extensively, owing to their especially efficient strong narrow-width emission band in the visible region.[14–16] In the last decade, a substantial amount of research has been devoted to design luminescent liquid crystals[17,18] to obtain the materials that combine the properties of liquid crystals and rare earth complexes.[19–21] Most examples of lanthanidomesogens are smectic liquid crystals,[22–24] which mimicked the disk-like or rod-like shape of the conventional organic liquid crystals[25] and some examples of lyotropic lanthanidomesogens have also been reported.[26,27] However, the high transition temperatures, unworkability, and low thermal stability are major drawbacks that hamper the application of the physical properties of these materials. Some methods have been put forward to overcome these problems such as by incorporating rare earth complexes into liquid crystalline polymers to obtain rare earth-containing LCPs materials. In addition rare earth-containing LCPs materials improved the promising applications in many fields such as optics, electronics, mechanics, displays, luminescent dye, and so forth.

In this paper, a series of new side-chain ChLCPs containing europium complexes were synthesized. The LC properties of the monomers and polymers obtained were characterized with differential scanning calorimetry (DSC), thermogravimetric analysis (TGA), polarizing optical microscopy (POM), and X-ray diffraction (XRD); the luminescent intensity and lifetimes were measured by fluorescence spectrophotometer. The influence of

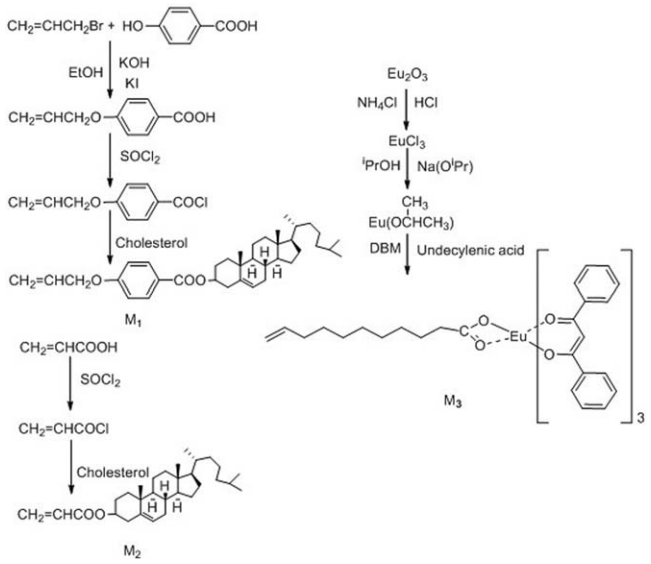

Figure 1. Synthesis routes of the olefinic monomers.

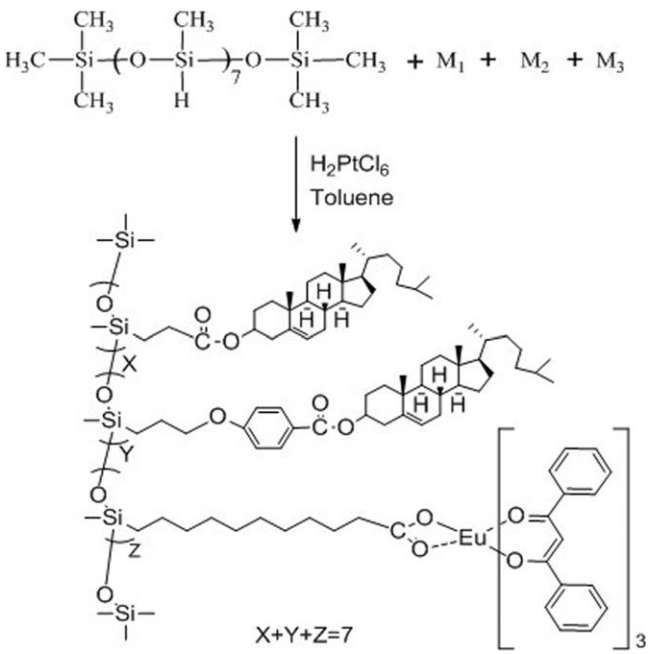

Figure 2. Synthesis routes of polymers.

the concentration of europium complexes units on phase behavior and optical properties were discussed.

EXPERIMENTAL

Instrumentation

Fourier transform infrared (FTIR) spectra was measured on a Nicollet 510 FTIR spectrometer (Nicollet Instruments, Madison); ^{1}H-NMR was measured by Varian WH-90PFT NMR Spectrometer (Varian Associates, Palo Alto, CA); element analyses (EA) were measured by Elementar Vario ELIII (Elementar, Germany); DSC and TGA measurements were carried out with a NETZSCH TGA 209C thermogravimetric analyzer, and a NETZSCH instruments DSC 204 (Netzsch, Wittelbacherstrasse, Germany) at a scanning rate of 10°C min^{-1} under a flow of dry nitrogen; The polarized optical microscopy (POM) study was performed using a Leica DMRX (Leica, Wetzlar, Germany) equipped with a Linkam THMSE-600 (Linkam, Surrey, England) heating stage; X-ray diffraction measurements were performed with a nickel-filtered Cu-Kα radiation with a DMAX-3A Rigaku powder diffractometer; Luminescence measurements were performed on a HORIBA Jobin Yvon FL3-TCSPC fluorescence spectrophotometer; IR imaging was performed using Spotlight 300 infrared imaging system (PerkinElmer).

Materials

Poly(methylhydrogeno)siloxane (PMHS, $M_n = 582$) was purchased from Jilin Chemical Industry Company (China); Bromopropene, 4-hydroxybenzoic acid, acrylic acid, undecylenic acid, 2-propanol, isopropoxide, and dibenzoylmethane (DBM) were purchased from Shenyang Chemical (China); Cholesterol was purchased from Henan Xiayi Medical (China); Eu_2O_3 was purchased from Beijing Fuxing Chemical Industry (China); Toluene was used in the hydrosilylation reaction over sodium and distilled under nitrogen. All other solvents were purified by standard methods.

Monomers Synthesis

The synthetic route to the olefinic monomers was shown in Figure 1, the liquid crystalline monomer cholesteryl 4-(allyloxy)-benzoate (M_1) was prepared according to previously reported synthetic method.[28]

Yield: 72%. IR (KBr): 3056 (=CH), 2973–2857 (–CH_3, –CH_2–), 1704 (C=O), 1643 (C=C), 1605, 1494 (Ar–), 1273, 1171 (C–O–C). $C_{37}H_{54}O_3$: Calcd. C 81.27, H 9.95; Found C 81.09, H 9.83. ^{1}H-NMR (600 MHz, $CDCl_3$, δ): 7.99–7.98 (d, J=9 Hz, 2H, Ar–H), 6.92 (d, J=9 Hz, 2H, Ar–H), 6.05 (m, 1H, CH_2=C**H**–), 5.44–5.41 (t, 2H, C**H**$_2$=CH–), 5.32–5.31 (m, 1H, =C**H**–in cholesteryl), 4.59–4.58 (d, J=4.8 Hz, 2H, –OCH_2–), 2.03–0.67 (m, 44H, cholesteryl–H).

Cholesteryl Acrylate M_2. 4.03 g (0.056 mol) of acrylic acid, 20 mL (0.27 mol) of thionyl chloride were added to a round-bottomed flask equipped with an absorption instrument of hydrogen chloride. The mixture was stirred at room temperature for 1 h, and then heated to 60°C for 5 h, the excess thionyl chloride was distilled under reduced pressure to obtain the acrylic acid chloride, Yield: 85%.

2.7 g (0.03 mol) of acrylic acid chloride was added dropwise to a cold solution of 11.58 g (0.03 mol) of cholesterol in 40 mL of chloroform and 2 mL of pyridine. The reaction mixture was heated to reflux for 12 h. The mixture was cooled to room temperature, poured into 200 mL of methanol. The precipitated crude product was filtered and recrystallized from ethanol.

Yield: 79%. IR (KBr): 3072 (=CH), 2972–2868 (–CH_3, –CH_2–), 1732 (C=O), 1636 (C=C). $C_{30}H_{48}O_2$: Calcd. C 81.76, H 10.98; Found C 81.57, H 11.13. ^{1}H-NMR (600 MHz, $CDCl_3$, δ): 6.40–5.78 (m, 2H, C**H**$_2$=CH–), 6.12–6.07 (m, 1H, CH_2=C**H**–), 5.38 (m, 1H, =C**H**–in cholesteryl), 3.77–3.74 (t, 1H, –COOCH– in cholesteryl), 1.64–0.67 (m, 43H, cholesteryl–H).

Eu($C_{11}H_{21}O_2$)(DBM)$_3$ M_3. Anhydrous europium chloride (2.58 g, 10.0 mmol), which was prepared from Eu_2O_3, ammonium

Table I. Polymerization and Yield

	Feed					
Polymer	PMHS (mmol)	M_1 (mmol)	M_2 (mmol)	M_3 (mmol)	Eu^{3+} (Mol %)	Yield (%)
P_1	0.25	1.050	0.7	0	0	87
P_2	0.25	1.047	0.698	0.005	0.3	77
P_3	0.25	1.043	0.696	0.011	0.6	85
P_4	0.25	1.040	0.694	0.016	0.9	81
P_5	0.25	1.037	0.692	0.021	1.2	86
P_6	0.25	1.034	0.690	0.026	1.5	73

Table II. Thermal Properties of Liquid Crystalline Monomers

Monomers	Phase transition temperature[a], °C (Corresponding enthalpy changes, J g^{-1})	Yield (%)	ΔT_1[b] (°C)	ΔT_2[c] (°C)
M_1	Heating: K 115.2 (43.10) Ch 248.6 (3.51) I	63	133.4	151.6
	Cooling: I 245.4 (0.78) Ch 93.8 (4.39) K			
M_2	Heating: K 84.8 (37.76) Ch 120.1 (0.59) I	67	35.3	72.9
	Cooling: I 117.6 (0.53) Ch 44.7 (4.39) K			

[a] Peak temperatures obtained by DSC were taken as the phase transition temperature.
[b] Mesophase temperature ranges on heating cycle.
[c] Mesophase temperature ranges on cooling cycle.
K, solid; Ch, cholesteric; I, isotropic.

chloride and hydrochloric acid,[29] was dissolved in 20 mL of benzene and anhydrous 2-propanol (1:1). The mixture was heated to 50°C for 12 h under N_2, and then this stirred solution was added a solution of sodium isopropoxide (2.46 g, 30.0 mmol) in 20 mL of 2-propanol.[30] The mixture was refluxed for 4 h to synthesize europium isopropoxide and a solution of dibenzoylmethane (6.72 g, 30.0 mmol) in 30 mL of benzene was added dropwise. After this solution was refluxed for 2.5 h, a solution of undecylenic acid (1.84 g, 10.0 mmol) in 20 mL of benzene was added. The reactive mixture was refluxed for 3 h. After cooling to room temperature, the mixture was filtered. The product was obtained after the solvent evaporated and washed three times with cyclohexane and dried under vacuum at room temperature for 12 h.

Yield: 59%. IR (KBr): 3059 (=CH), 2924–2852, 1452 (–CH_2–), 1641 (C=C), 1601, 1479 (Ar–), 1597 (C=O), 1552 (–COO–), 432 (Eu–O). $C_{56}H_{55}O_8$ Eu: Calcd. C 78.60, H 6.43, Eu 15.09; Found C 78.53, H 6.51, Eu 14.91. ^{1}H-NMR (600 MHz, DMSO, δ): 7.65–7.11 (m, 6H, Ar–H), 6.80 (m, 12H, Ar–H), 6.64–6.37 (m, 12H, Ar–H), 5.65 (m, 1H, CH_2=C**H**$(CH_2)_8$–), 4.89–4.84 (m, 2H, C**H**$_2$=CH$(CH_2)_8$–), 3.73 (s, 6H, –CH_2– in DBM), 2.98 (m, 2H, –C**H**$_2$COO–) 1.34–0.72 (m, 14H, –$(CH_2)_7$–).

Synthesis of the Liquid Crystalline Polymers

For synthesis of all the polymers, a standard method was adopted, as shown in Figure 2. The polymerization experiments were summarized in Table I. The synthesis of P_4 was presented as an example. Liquid crystalline monomers M_1 (0.538 g, 0.987 mmol), M_2

Table III. DSC, POM, and TGA Results of the Series of Polymers

	DSC			POM		TG
Sample	T_g (°C)	T_i (°C)	ΔT[a]	T_{i1}[b] (°C)	T_{i2}[c] (°C)	$T_{0.5\%}$[d] (°C)
P_1	36.1	173.7	137.6	180.3	178.7	305.2
P_2	38.4	169.9	131.7	173.2	171.4	302.8
P_3	39.7	169.1	129.4	171.7	169.3	309.6
P_4	39.1	165.6	126.5	169.9	167.5	302.3
P_5	40.4	162.2	121.8	166.5	164.6	311.6
P_6	41.3	160.1	118.8	163.3	161.9	307.3

[a] Mesophase temperature ranges ($T_i - T_g$).
[b] Temperature at which the birefringence disappeared completely.
[c] Temperature at which the mesophase occurred.
[d] Temperature at which 5% weight loss occurred.

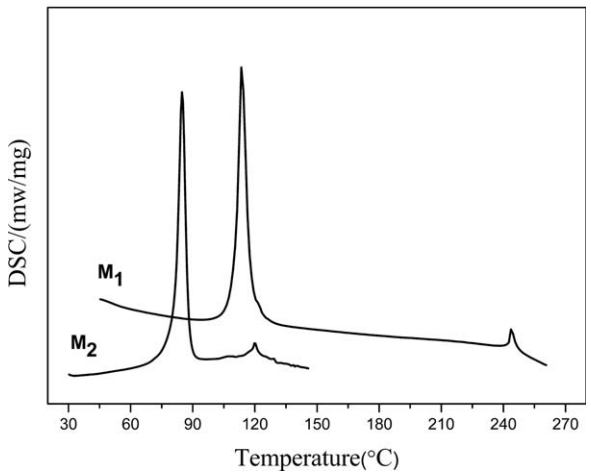

Figure 3. DSC thermograms of liquid crystalline monomers.

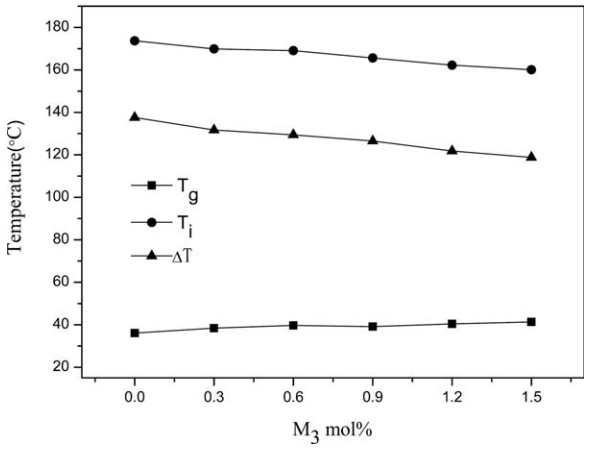

Figure 5. Effect of M_3 content on phase transition temperatures.

(0.290 g, 0.658 mmol) were dissolved in 40 mL of dry, freshly distilled toluene. To the stirred solution, europium complexes monomer M_3 (0.105 g, 0.105 mmol), PMHS (0.145 g, 0.25 mmol) and 1.5 mL of H_2PtCl_6 in 30 mL THF were added, the mixture was heated under nitrogen and anhydrous conditions at 65°C for 72 h. Then the solution was cooled and poured into 150 mL methanol, after filtration, the product was washed with hot ethanol (three times), and dried at 80°C under vacuum for 12 h to obtain polymer P_4.

Yield: 81%. IR (KBr,): 2927–2853 ($-CH_3$, $-CH_2-$), 1745–1731 (C=O), 1605, 1510 (Ar), 1211 (C–O–C), 1128–1007 (Si–O–Si).

RESULTS AND DISCUSSION

Syntheses

The synthetic routes for the target monomers and polymers were shown in Figures 1 and 2, the chemical structures of monomers and polymers were characterized by FTIR and ^{1}H-NMR spectroscopy. The FTIR spectra of M_1 and M_2, respectively, showed characteristic bands for ester C=O stretching (1730–1740 cm^{-1}), olefinic C=C stretching (1635–1645 cm^{-1}), and aromatic C=C stretching (1605–1510 cm^{-1}) in good agreement with the prediction. The FTIR spectra of M_3 showed characteristic bands for olefinic C=C stretching (1641 cm^{-1}), aromatic C=C stretching (1601–1479 cm^{-1}), β–diketone C=O stretching (1597 cm^{-1}), and Eu–O stretching (432 cm^{-1}) in good agreement with the prediction. The ^{1}H-NMR spectra of M_1 and M_2, respectively, showed peaks at 7.99–6.37, 6.40–4.84, and 2.43–0.67 ppm corresponding to aromatic, olefinic protons, and methyl and methylene protons, respectively.

The polymers were synthesized by a one-step hydrosilylation reaction between Si–H groups of PMHS and olefinic C=C of monomers in toluene, using hexachloroplatinic acid as catalyst at 65°C. The reaction was monitored following the disappearance of the Si–H band at 2166 cm^{-1} in the FTIR spectra. The completely disappearance of the Si–H band indicated successful incorporation of monomers into the polysiloxane chains. Yields and detailed polymerization were summarized in Table I. All the polymers were characterized by FTIR spectroscopy. Polymer P_4 contained the representative features for all of the polymers. The characteristic absorption bands were as follows: 2927–2853 cm^{-1} (C–H stretching), 1745–1731 cm^{-1} (C=O stretching), 1605, 1510 cm^{-1} (C=C stretching of aromatic nucleus), 1211 cm^{-1} (C–O stretching), and 1128–1007 cm^{-1} (Si–O stretching).

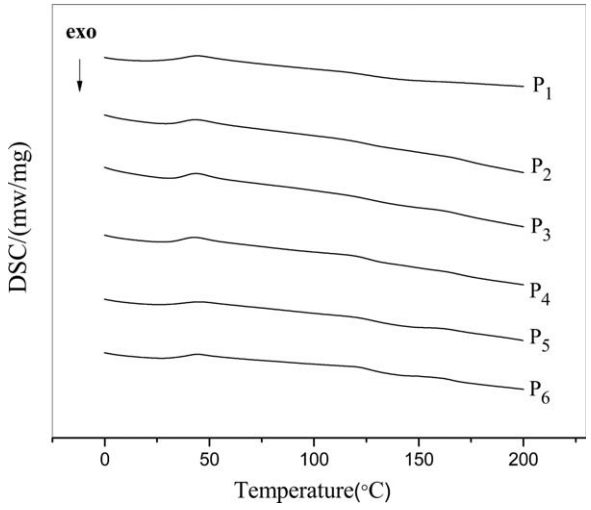

Figure 4. DSC thermograms of polymers.

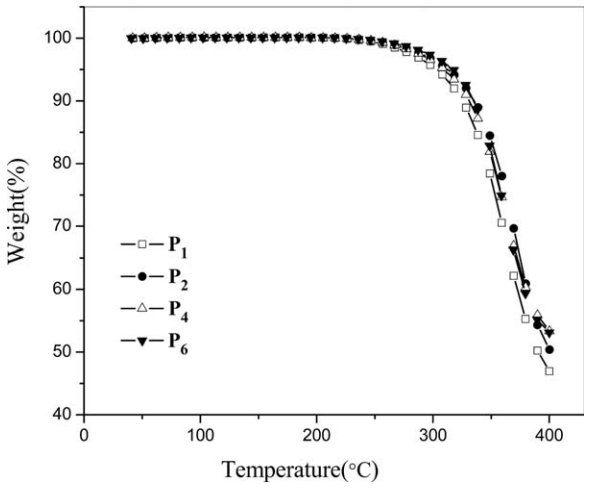

Figure 6. TGA curves of representative polymers.

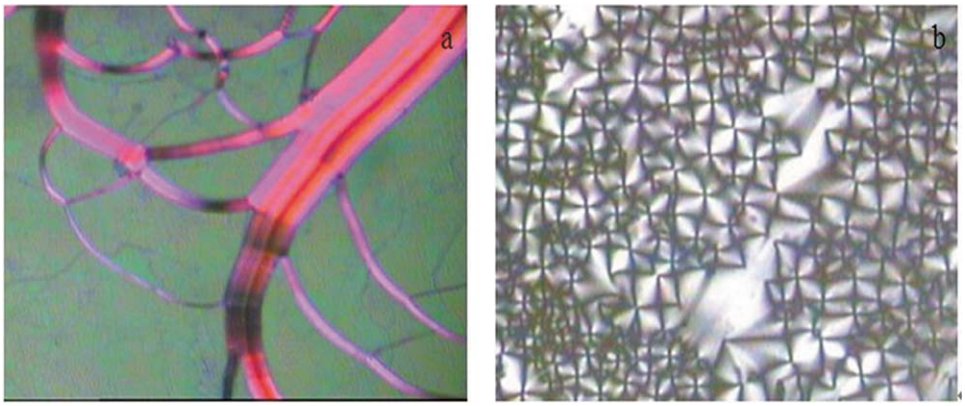

Figure 7. Optical texture of monomers (200×): (a) oily streaks texture of M_1 on heating to 150°C; (b) focal-conic texture of M_2 on cooling to 106.4°C. [Color figure can be viewed in the online issue, which is available at wileyonlinelibrary.com.]

Thermal Properties

The thermal properties of liquid crystalline monomers and polymers were determined by DSC, POM and TGA (Tables II and III). Thermal properties determined by DSC were consistent with POM observation results. Typical DSC curves of liquid crystalline monomers and polymers were shown in Figures 3 and 4, respectively.

DSC thermograms of LC monomers M_1 and M_2 showed: an endothermic melting transition at 115.2°C for M_1 and 84.8°C for M_2; an endothermic mesogenic–isotropic phase transition at 248.6°C for M_1 and 120.1°C for M_2; an isotropic to LC phase transition at 189.4°C for M_1 and 117.6°C for M_2, and crystallization temperature at 93.8°C for M_1 and 44.7°C for M_2 on the first cooling.

All the polymers synthesized showed a glass transition at low temperatures and a LC phase to isotropic transition at high temperature. For all the polymers, reversible mesomorphic phase transitions were observed due to sufficient liquid crystalline molecular motion and orientation suggesting that physical cross-linking of europium complexes units did not disturb the liquid crystalline order of the polymer systems.

The tested range of europium complexes unit concentrations in polymers P_2–P_6 did not significantly affect the glass transition of polymers on heating cycles ($\Delta T_g = 5$°C); however they had obvious influence on the mesophasic-to-isotropic transition with T_i decreasing by 14°C (Table 3; Figure 5). Low temperatures induced vitrification rather than crystallization[31] due the intrinsic disordered and atactic systems of the side-chains of the

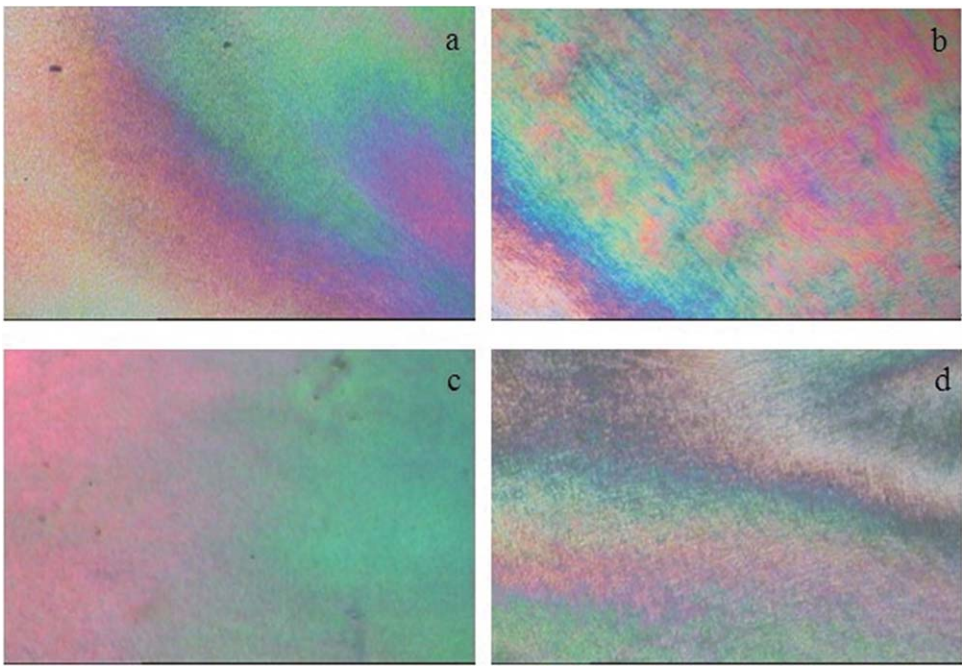

Figure 8. Optical textures of monomers (200 ×): (a) Grandjean texture of P_1 at heating to 150°C; (b) Grandjean texture of P_3 at heating to 110°C; (c) Grandjean texture of P_5 at heating to 110°C; (d) Grandjean texture of P_5 at cooling to 123°C. [Color figure can be viewed in the online issue, which is available at wileyonlinelibrary.com.]

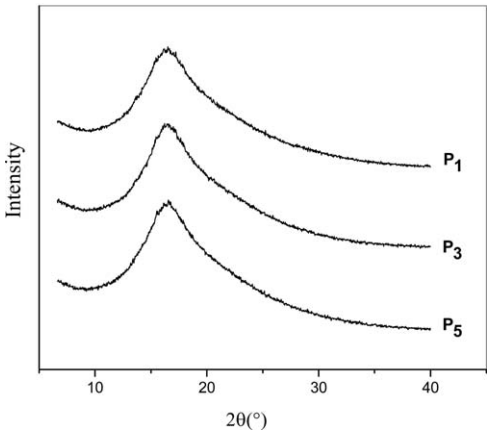

Figure 9. XRD curves of representative polymers at 125°C.

siloxane containing liquid crystalline. The flexible side chains interacted with the mesogenic rigid moieties and with europium complexes units; thus influenced the mesophase behaviors of the polymers. The glass transition temperature (T_g) may be considered as a measure of the backbone flexibility. For polymers with a low content of europium complexes units, the glass transition temperature was not significantly affected indicating that the backbone flexibility did not change significantly. On the other, hand increasing concentration of europium complexes units (0–1.5 mol %), destroyed the regularity of chain segments, disturbing the liquid crystalline molecular mobility and orientation. The result was a decrease in temperature from the mesophasic to isotropic transition. In short, the introduction of europium complexes units did not change the liquid crystalline state of the polymer systems.

TGA results showed that the temperatures at which 5% weight loss occurred (T_d) were greater than 300°C for all the polymers, as shown in Figure 6, this indicated that the synthesized polymers had good thermal stability.

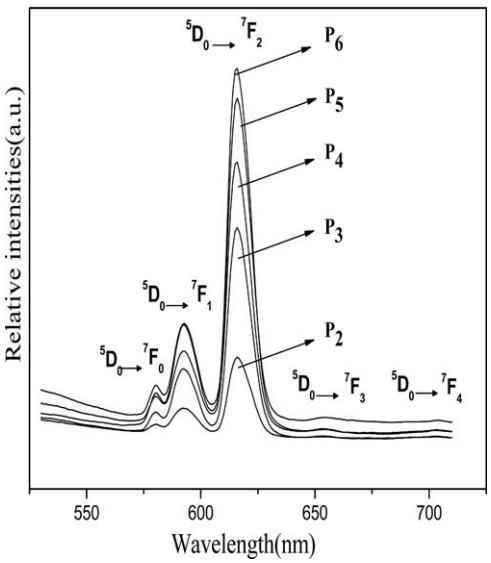

Figure 10. Emission spectra of P_2–P_6; all the transitions in the emission spectrum start from the $^5D_0$ state and end at the ^7F_J levels ($J = 0$–4).

Optical Texture

The optical textures of the monomers and polymers were studied by use of POM with variable temperature test bench under nitrogen atmosphere. POM observations showed that the monomers M_1 and M_2 exhibited enantiotropic oily-streak texture and focal–conic texture of the cholesteric phase during the heating and cooling cycles. When M_1 was heated to 114°C, the sample began to melt, the typical cholesteric oily streak texture gradually appeared, and the texture disappeared at 249°C. When the isotropic state was cooled to 245°C, the focal-conic texture appeared. When M_2 was heated to 84°C, the sample began to melt, the typical cholesteric oily streak texture gradually appeared, and the texture disappeared at 121°C. When the isotropic state was cooled to 118°C, the focal-conic texture appeared. Photomicrographs of M_1 and M_2 are shown in Figure 7(a,b).

All of the polymers showed similar cholesteric phase textures in the heating and cooling cycles. When P_5 here used as example was heated to 48°C, the cholesteric Grandjean texture gradually appeared, and the selective reflection color changed from red to blue with increasing temperature; the texture disappeared at 166.5°C. Similarly when the isotropic state was cooled to 164.6°C the similar cholesteric Grandjean texture gradually appeared. Photomicrographs of P_1, P_3, and P_5 were shown in Figure 8(a–d).

The cholesteric mesophase of polymers was also confirmed by X-ray diffraction. XRD studies were carried out to obtain more detailed information on LC phase structure. All the polymers displayed broad peaks at wide angles around $2\theta \approx 17°$ in the wide-angle region of XRD measurement and a sharp peak associated with the smectic layers did not appear in the small-angle region of XRD measurement. Therefore, cholesteric phase structure of polymers was confirmed by X-ray diffraction, which was consistent with DSC and POM results. Figure 9 showed the representative X-ray diffraction diagrams of samples P_1, P_3, and P_5 at 125°C.

Luminescent Properties

By quick freezing the obtained polymers P_2–P_6 in the LC phases in liquid nitrogen vitrified mesophase solids were obtained and the luminescent properties of the LC states were examined. Representative photoluminescence spectra of polymers were given in Figure 10 and the detailed luminescent data were shown in Table IV.

Narrow-wide red emissions were observed. The emission spectra showed the characteristic $^5D_0 \rightarrow {}^7F_j$ (j= 0, 1, 2, 3, 4) transitions of Eu^{3+}. The band near 579 nm was assigned to the $^5D_0 \rightarrow {}^7F_0$ transition; the bands near 592 nm was assigned to the $^5D_0 \rightarrow {}^7F_1$ transitions; the bands near 612 nm was assigned to the $^5D_0 \rightarrow {}^7F_2$ transitions; the band near 653 nm was assigned to the $^5D_0 \rightarrow {}^7F_3$ transition; and the bands near 702 nm was assigned to the $^5D_0 \rightarrow {}^7F_4$ transitions. The maxima of these bands were sourced from $^5D_0 \rightarrow {}^7F_1$ and $^5D_0 \rightarrow {}^7F_2$ transitions, respectively. It was common knowledge that the $^5D_0 \rightarrow {}^7F_0$ transition of Eu^{3+} was strictly prohibited in a symmetric field, so the existence of this band indicates that Eu^{3+} in polymers was in low symmetry and did not have an inversion center. The $^5D_0 \rightarrow {}^7F_1$ transition was a magnetic dipolar transition; its intensity hardly changes with the local

Table IV. Luminescent Property Data of P_2–P_6

Sample	Excitation bands (nm)	Emission bands (nm)	Relative intensities[a]	τ[b] (ms)
P_2	370	580, 592, 616, 650, 703	32.0, 56.7, 134.7, 13.2, 13.3	0.455
P_3	370	579, 592, 616, 653, 702	50.7, 116.6, 332.0, 14.3, 13.9	0.473
P_4	370	579, 591, 615, 653, 702	75.1, 143.8, 431.6, 24.3, 22.8	0.493
P_5	370	579, 593, 615, 653, 703	79.7, 184.0, 529.2, 25.3, 23.9	0.509
P_6	370	580, 594, 615, 653, 704	91.9, 186.1, 574.7, 42.6, 25.0	0.530

[a] Relative intensities were obtained by the calculation of the integral area of the same emission bands.
[b] For the $^5D_0 \rightarrow {}^7F_2$ transition of Eu^{3+}.

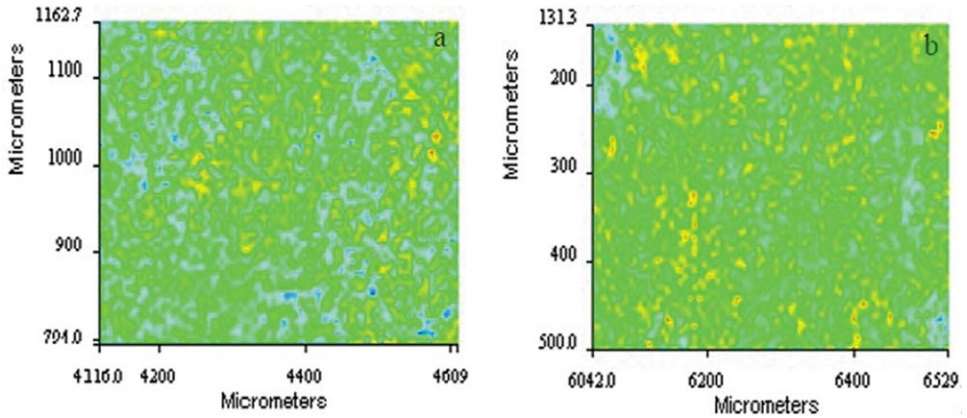

Figure 11. IR imaging of P_2 (a) and P_6 (b). [Color figure can be viewed in the online issue, which is available at wileyonlinelibrary.com.]

structural environment. On the other hand, the $^5D_0 \rightarrow {}^7F_2$ transition was an electric dipole transition and was sensitive to the coordination environment of the Eu^{3+}. Figure 10 showed that when Eu^{3+} ion content increases the luminescent intensity of the polymers gradually increases accordingly. At Eu^{3+} (mol %) = 1.5%, P_6 still did not show fluorescence quenching, possibly due to the introduction of PMHS. With the introduction of PMHS, europium complexes units can be evenly distributed in the polymers, thus preventing the europium complexes units' close and aggregation. This result can be explained by IR imaging analysis, the IR imaging of P_2 and P_6 were shown in Figure 11(a,b). The yellow zone represented the europium complexes units and corresponds to the carboxylate characteristic peak at 1552 cm^{-1}. Figure 11 showed that the europium complexes units evenly distributed in P_2 and P_6, rather than gather together to form clusters. Therefore, it was difficult to reach Eu^{3+} ions concentration able to quench the fluorescence. This was confirmed by the values of the intensity ratios of the $^5D_0 \rightarrow {}^7F_2$ to $^5D_0 \rightarrow {}^7F_1$ transitions which were 2.38, 2.85, 3, 3.37, and 3.09 respectively. These ratio values are only possible when the Eu^{3+} ions did not occupy a site with inversion symmetry.[32,33]

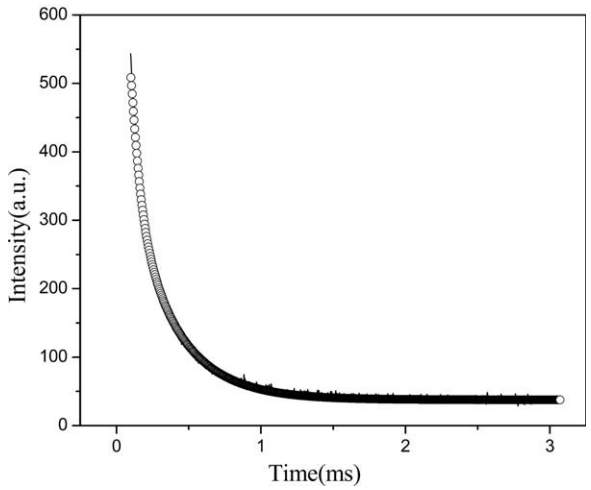

Figure 12. Decay curves of P_3 (open circles, experimental data; solid line, curve fitting, fitted according to $I = I_0 + A \exp[-(t - t_0)/\tau]$).

The typical decay curves of the Eu^{3+} ion in polymers and M_3 were measured, and the luminescence decay curves were all single exponential, confirming that all Eu^{3+} ion lie in the same average coordination environment. The resulting lifetimes of europium materials were included in Table IV. The decay curve of P_3 was presented as example (Figure 12). The data showed that luminescent lifetimes were greater than 0.45 ms for all the polymers. In addition, with Eu^{3+} ion content increases, the luminescent lifetimes of the polymers were extended slightly. This indicated that the content of Eu^{3+} ion in polymers had a small influence on the lifetime of the Europium-containing ChLCPs materials.

CONCLUSIONS

In this article, monomers M_1 and M_2 exhibited cholesteric oily-streak texture and focal-conic texture, The TGA results showed that 5% weight loss temperatures were greater than 300°C for all polymers. With an increase of europium complexes unit in the polymers, the glass transition temperature (T_g) do not change significantly; the isotropic temperature (T_i) and mesophase temperature range (ΔT) decreased. All the polymers showed typical cholesteric grandjean textures when it was heated and cooled, which were confirmed by X–ray diffraction, the polymers displayed broad peaks at wide angles around $2\theta \approx 17°$ and a sharp peak associated with the smectic layers did not appear in the small-angle region of XRD measurement. With Eu^{3+} ion contents ranging between 0 and 1.5 mol %, luminescent intensity of polymers gradually increased and luminescent lifetimes were longer than 0.45 ms for the polymers. These results indicated that the introduction of europium complexes units did not change the liquid crystalline state of the polymer systems, while the polymers were enabled with the significant luminescent properties.

ACKNOWLEDGMENTS

The authors are grateful to the National Natural Science Fundamental Committee of China, the HI-Tech Research and Development Program (863) of China, the National Basic Research Priorities Program (973) of China for financial support of this work.

REFERENCES

1. Stohr, A.; Strohriegl, P. *Macromol. Chem. Phys.* **1998**, *199*, 751.
2. Pfeuffer, T.; Kürschner, K.; Strohriegl, P. *Macromol. Chem. Phys.* **1999**, *200*, 2480.
3. Liu, J.-H.; Yang, P.-C. *Polymer* **2006**, *47*, 4925.
4. Andreu, R.; Espinosa, M.; Galia, M.; Cadiz, V.; Ronda, J.; Reina, J. *J. Polym. Sci., Part A: Polym. Chem.* **2006**, *44*, 1529.
5. Oriol, L.; Pinol, M.; Serrano, J.; Martınez, C.; Alcalá, R.; Cases, R.; Sánchez, C. *Polymer* **2001**, *42*, 2737.
6. Gopalan, P.; Andruzzi, L.; Li, X.; Ober, C. K. *Macromol. Chem. Phys.* **2002**, *203*, 1573.
7. Meng, F.; Zhang, B.; Liu, L.; Zang, B. *Polymer* **2003**, *44*, 3935.
8. Bunning, T.; Kreuzer, F.-H. *Trends Polym. Sci.* **1995**, *3*, 318.
9. Hsu, C. S.; Percec, V. *J. Polym. Sci. Part A: Polym. Chem.* **1989**, *27*, 453.
10. Lub, J.; Broer, D.; Hikmet, R.; Nierop, K. *Liq. Cryst.* **1995**, *18*, 319.
11. Hikmet, R.; Lub, J.; Higgins, J. *Polymer* **1993**, *34*, 1736.
12. Walba, D. M.; Yang, H.; Shoemaker, R. K.; Keller, P.; Shao, R.; Coleman, D. A.; Jones, C. D.; Nakata, M.; Clark, N. A. *Chem. Mater.* **2006**, *18*, 4576.
13. Slooff, L.; van Blaaderen, A.; Polman, A.; Hebbink, G.; Klink, S.; Van Veggel, F.; Reinhoudt, D.; Hofstraat, J. *J. Appl. Phys.* **2002**, *91*, 3955.
14. Lenaerts, P.; Driesen, K.; Van Deun, R.; Binnemans, K. *Chem. Mater.* **2005**, *17*, 2148.
15. Yan, B.; Qiao, X.-F. *J. Phys. Chem. B* **2007**, *111*, 12362.
16. Yan, B.; Lu, H.-F. *Inorg. Chem.* **2008**, *47*, 5601.
17. Suárez, S.; Imbert, D.; Gumy, F.; Piguet, C.; Bünzli, J.-C. G. *Chem. Mater.* **2004**, *16*, 3257.
18. Bünzli, J.-C. G.; Piguet, C. *Chem. Soc. Rev.* **2005**, *34*, 1048.
19. Binnemans, K.; Görller-Walrand, C. *Chem. Rev.* **2002**, *102*, 2303.
20. Knyazev, A. A.; Galyametdinov, Y. G.; Goderis, B.; Driesen, K.; Goossens, K.; Görller-Walrand, C.; Binnemans, K.; Cardinaels, T. *Eur. J. Inorg. Chem.* **2008**, 2008, 756.
21. Yin, S.; Sun, H.; Yan, Y.; Li, W.; Wu, L. *J. Phys. Chem. B* **2009**, *113*, 2355.
22. Binnemans, K.; Lodewyckx, K. *Angew. Chem.* **2001**, *113*, 248.
23. Escande, A.; Guénée, L.; Nozary, H.; Bernardinelli, G.; Gumy, F.; Aebischer, A.; Bünzli, J. C. G.; Donnio, B.; Guillon, D.; Piguet, C. *Chem. Eur. J.* **2007**, *13*, 8696.
24. Guillet, E.; Imbert, D.; Scopelliti, R.; Bünzli, J.-C. G. *Chem. Mater.* **2004**, *16*, 4063.
25. Binnemans, K. *J. Mater. Chem.* **2009**, *19*, 448.
26. Selivanova, N. M.; Galeeva, A. I.; Gubaydullin, A. T.; Lobkov, V. S.; Galyametdinov, Y. G. *J. Phys. Chem. B* **2012**, *116*, 735.
27. Zhang, T.; Spitz, C.; Antonietti, M.; Faul, C. F. *Chem. Eur. J.* **2005**, *11*, 1001.
28. Hu, J. S.; Zhang, B. Y.; Pan, W.; Li, Y. H.; Ren, S. C. *J. Appl. Polym. Sci.* **2006**, *99*, 2330.
29. Taylor, M.; Carter, C. *J. Inorg. Nucl. Chem.* **1962**, *24*, 387.
30. Wang, L.-H.; Wang, W.; Zhang, W.-G.; Kang, E.-T.; Huang, W. *Chem. Mater.* **2000**, *12*, 2212.
31. Zhang, B.-Y.; Meng, F.-B.; Li, Q.-Y.; Tian, M. *Langmuir* **2007**, *23*, 6385.
32. Capobianco, J.; Proulx, P.; Bettinelli, M.; Negrisolo, F. *Phys. Rev. B: Condens. Matter* **1990**, *42*, 5936.
33. Bu, W.; Li, H.; Li, W.; Wu, L.; Zhai, C.; Wu, Y. *J. Phys. Chem. B* **2004**, *108*, 12776.